Supporting information

H_2O_2 oxidation of cysteine residues in c-Jun N-terminal kinase 2 (JNK2) contributes to redox regulation in human articular chondrocytes

Kimberly J. Nelson[1], Jesalyn A. Bolduc[2], John Collins[2], Elizabeth A. Burke[3], Julie A. Reisz[3], Chananat Klomsiri[1,3], Scott T. Wood[2], Raghunatha R. Yammani[3], Leslie B. Poole[1], Cristina M. Furdui[3], and Richard F. Loeser[2,*]

[1]Department of Biochemistry, Wake Forest School of Medicine, Winston-Salem, NC, USA.
[2]Division of Rheumatology, Allergy and Immunology and the Thurston Arthritis Research Center, University of North Carolina at Chapel Hill, Chapel Hill, NC, USA.
[3]Department of Internal Medicine, Section on Molecular Medicine, Wake Forest School of Medicine, Winston-Salem, NC, USA.

Contents:

Table S1. Cysteine oxidation events identified by LC-MS/MS analysis

	Experiment 1 (DTT present, free thiols trapped with IAM, no disulfide analysis)		**Experiment 2 (pre-reduced JNK, free thiols trapped with MSBT, disulfide analysis)**	
	DTT 0 μM H_2O_2	**DTT 5 × 100 μM H_2O_2**	**DTT**	**100 μM H_2O_2**
C6	IAM	IAM	MSBT	MSBT SO_2H (Fig. S6A)
C41	IAM	IAM	MSBT	N.D.[1]
C79	IAM	IAM	N.D.[1]	MSBT
C116	IAM SO_2H (Fig. S6B) SO_3H (Fig. S6C)	IAM SO_2H (Fig. S6B) SO_3H (Fig. S6C)	N.D.[1]	SH
C137	IAM	IAM	MSBT	MSBT
C163	IAM	IAM	MSBT	MSBT SO_2H (Fig. S6D)
C177	SH (Fig. S4)	SH (Fig. S4)	MSBT SO_2H (Fig. S6E) SO_3H (Fig. S6F)	MSBT SO_2H (Fig. S6E) SO_3H (Fig. S6F)
C213	IAM	IAM SO_3H (Fig. S6G)	MSBT	MSBT
C222	IAM	IAM dimedone (Fig. S5)	MSBT (Fig. 4A) SO_2H (Fig. S6H) SO_3H (Fig. S6I) dimedone (Fig. 4A)	MSBT (Fig. 4A) SO_2H (Fig. S6H) SO_3H (Fig. S6I) dimedone (Fig. 4A)
C423	N.D.[1]	N.D.[1]	N.D.[1]	N.D.[1]
disulfides	Not measured[2]	Not measured[2]	0 disulfides detected	2 disulfides detected C222-C213 (Fig S7A) C222-C177 (Fig. S7B)

[1]Not detected

[2]Excess DTT present in the assay did not allow for detection of disulfide bonds

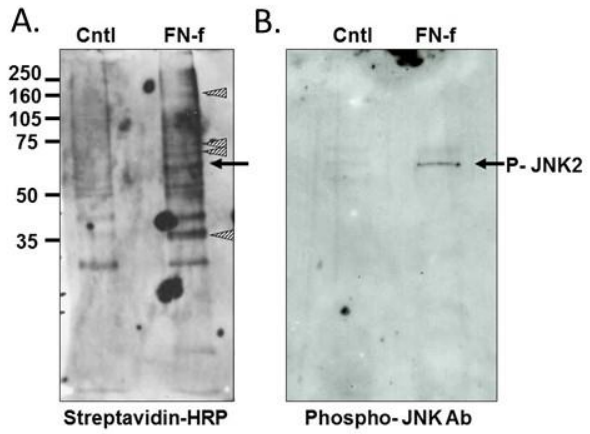

Fig. S1. JNK2 is oxidized upon chondrocyte FN-f stimulation. Chondrocytes were stimulated for 45 min with fibronectin fragment (FN-f) or control (Cntl) media. A biotin-labeled dimedone analog (DCP-Bio1) was added to the cell lysis buffer in order to label sulfenic acid-containing proteins. DCP-Bio1 labeled proteins were enriched using streptavidin-linked beads and separated by SDS-PAGE. Affinity-captured proteins were visualized by: **(A)** immunoblotting with streptavidin-HRP and **(B)** anti-phospho-JNK Ab. Black arrows indicate the expected protein band for JNK2 and striped arrowheads indicate additional proteins affinity captured after FN-f stimulation.

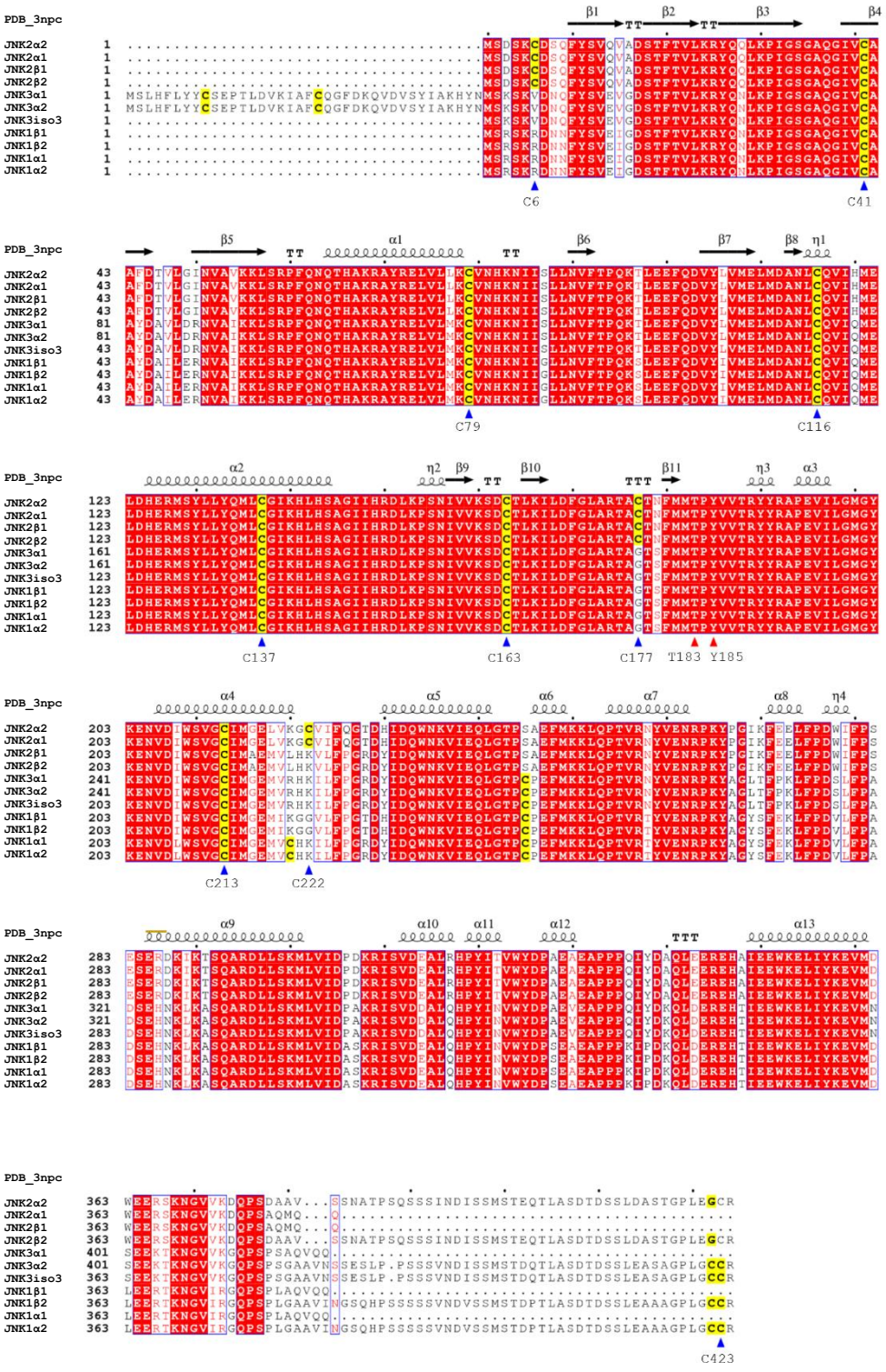

Fig. S2. Sequence alignment of human JNK isoforms. JNK sequences were aligned using Clustal Omega(1). Cysteine residues are highlighted in yellow. Cysteine residues and phosphorylation sites in JNK2 are indicated with blue and pink arrows, respectively.

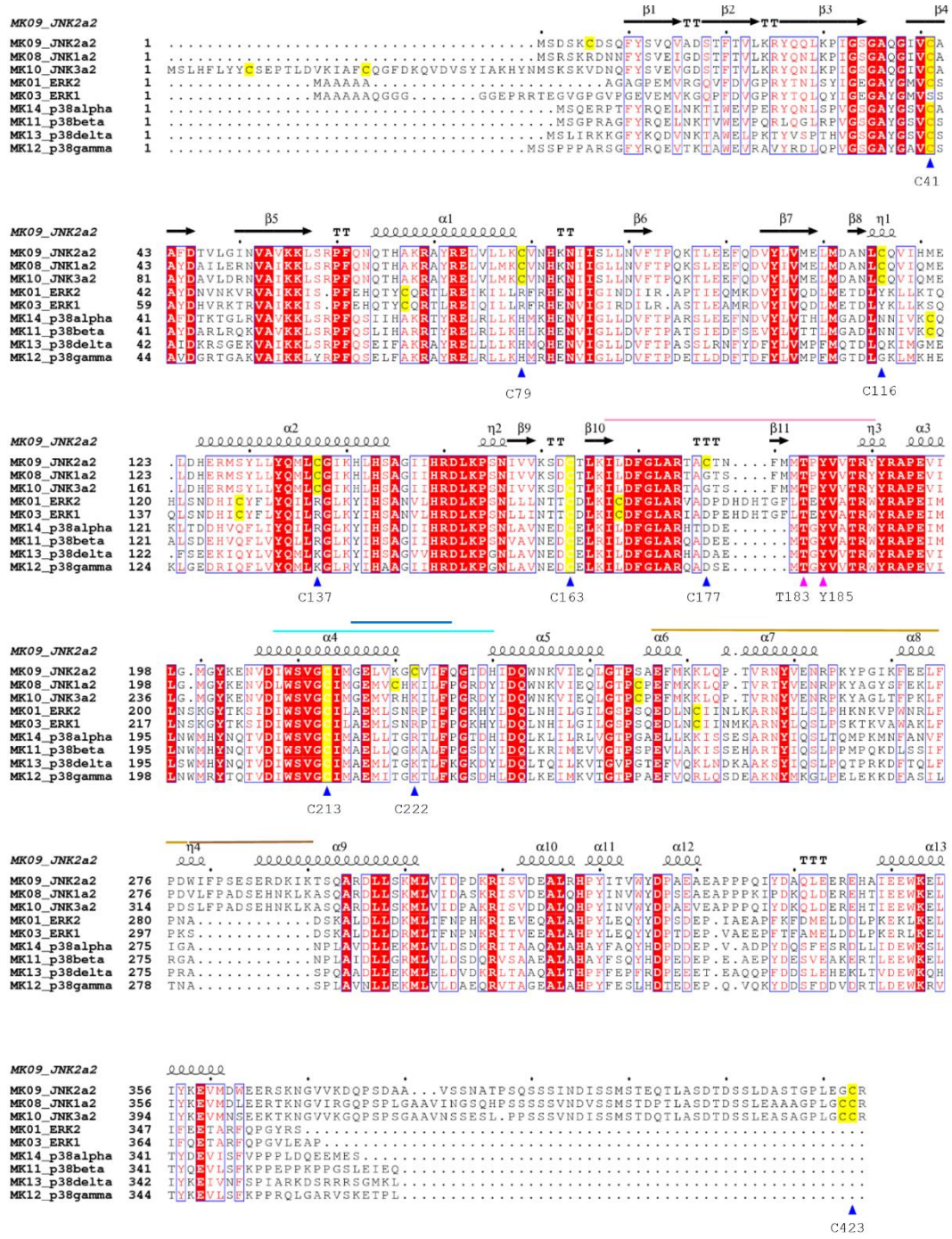

Fig. S3. Sequence alignment of human MAP kinases. MAP kinase sequences (Genbank accession numbers: NP_002743.3, NP_620707.1, NP_620708.1, NP_620709.1, NP_620634.1, NP_001310231.1, NP_001265476.1, NP_620637.1, NP_620448.1, NP_002744.1, NP_620407.1, NP_002737.2, NP_002960.2, NP_620581.1, NP_002745.1, NP_002742.3) were aligned using Clustal Omega(1). Cysteine residues are highlighted in yellow. Cysteine residues and phosphorylation sites in JNK2 are indicated with blue and pink arrows, respectively. Important functional regions of the JNK structure are indicated with lines above the alignment including the JNK2 substrate specificity-determining region (2) in cyan, the α-region(3) in blue, the activation loop in pink, the MAP kinase insert in tan, and the JNK insert in brown.

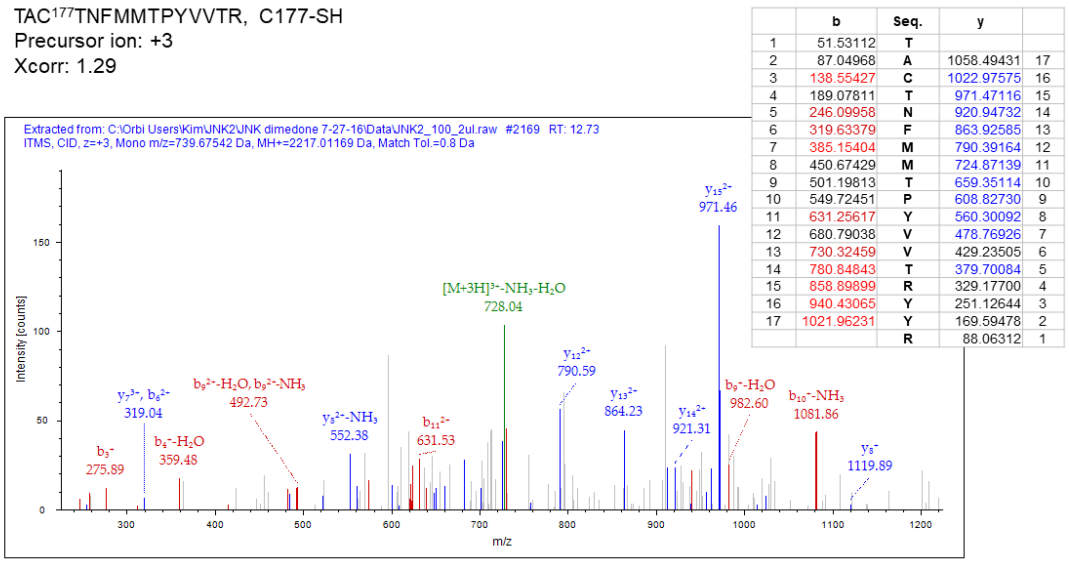

	b	Seq.	y	
1	51.53112	T		
2	87.04968	A	1058.49431	17
3	138.55427	C	1022.97575	16
4	189.07811	T	971.47116	15
5	246.09958	N	920.94732	14
6	319.63379	F	863.92585	13
7	385.15404	M	790.39164	12
8	450.67429	M	724.87139	11
9	501.19813	T	659.35114	10
10	549.72451	P	608.82730	9
11	631.25617	Y	560.30092	8
12	680.79038	V	478.76926	7
13	730.32459	V	429.23505	6
14	780.84843	T	379.70084	5
15	858.89899	R	329.17700	4
16	940.43065	Y	251.12644	3
17	1021.96231	Y	169.59478	2
		R	88.06312	1

Fig. S4. Positive ion MS2 spectrum of the reduced C177 peptide. Spectra were obtained after treating recombinant His-tagged JNK2α2 with and without 5 additions of 100 μM H_2O_2 in the presence of 5 mM DTT and 5 mM dimedone (Table SI, Experiment 1). Free thiols were blocked with IAM prior to digestion with trypsin. The resulting peptides were analyzed by LC-MS/MS using an Accela Open UPLC coupled to a Thermo Scientific Orbi-trap LTQ XL mass spectrometer.

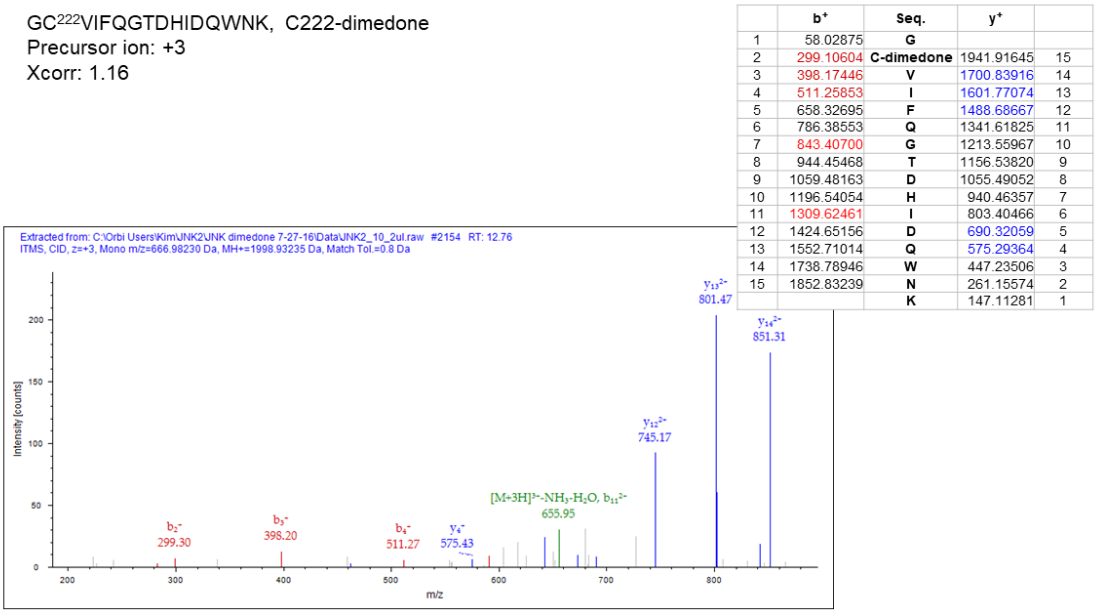

	b+	Seq.	y+	
1	58.02875	G		
2	299.10604	C-dimedone	1941.91645	15
3	398.17446	V	1700.83916	14
4	511.25853	I	1601.77074	13
5	658.32695	F	1488.68667	12
6	786.38553	Q	1341.61825	11
7	843.40700	G	1213.55967	10
8	944.45468	T	1156.53820	9
9	1059.48163	D	1055.49052	8
10	1196.54054	H	940.46357	7
11	1309.62461	I	803.40466	6
12	1424.65156	D	690.32059	5
13	1552.71014	Q	575.29364	4
14	1738.78946	W	447.23506	3
15	1852.83239	N	261.15574	2
		K	147.11281	1

Fig. S5. Positive ion MS2 spectrum of the dimedone-labeled C222 peptide. Spectra were obtained after treating recombinant His-tagged JNK2α2 with and without 5 additions of 100 µM H_2O_2 in the presence of 5 mM DTT and 5 mM dimedone (Table SI, Experiment 1). Free thiols were blocked with IAM prior to digestion with trypsin. The resulting peptides were analyzed by LC-MS/MS using an Accela Open UPLC coupled to a Thermo Scientific Orbi-trap LTQ XL mass spectrometer.

A.

C[6]DSQFYSVQVADSTFTVLK, C6-Dioxidation
Precursor Ion: +3
XCorr: 2.54

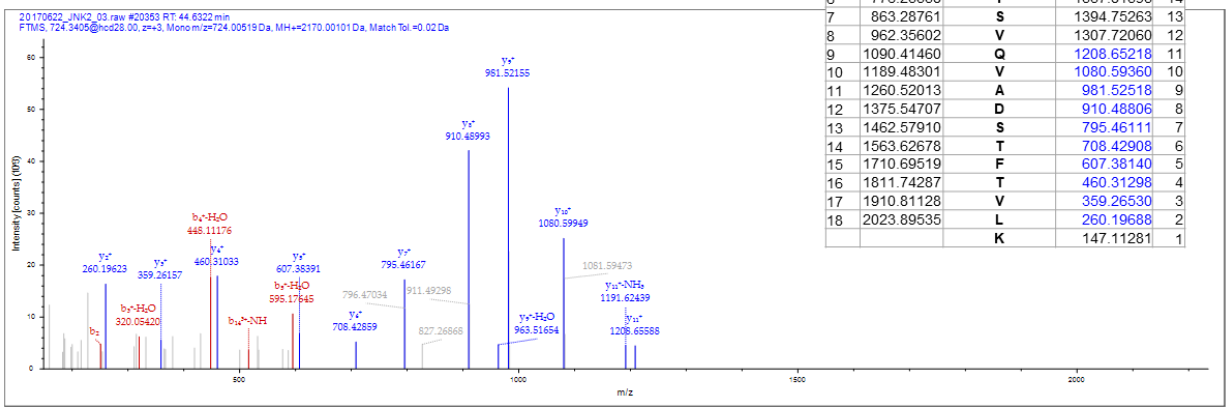

	b+	Seq.	y+	
1	136.00629	C-Dioxidation		
2	251.03323	D	2035.00193	18
3	338.06526	S	1919.97498	17
4	466.12384	Q	1832.94295	16
5	613.19225	F	1704.88437	15
6	776.25558	Y	1557.81595	14
7	863.28761	S	1394.75263	13
8	962.35602	V	1307.72060	12
9	1090.41460	Q	1208.65218	11
10	1189.48301	V	1080.59360	10
11	1260.52013	A	981.52518	9
12	1375.54707	D	910.48806	8
13	1462.57910	S	795.46111	7
14	1563.62678	T	708.42908	6
15	1710.69519	F	607.38140	5
16	1811.74287	T	460.31298	4
17	1910.81128	V	359.26530	3
18	2023.89535	L	260.19688	2
		K	147.11281	1

B.

TLEEFQDVYLVM[108]ELM[111]DANLC[116]QVIHM[121]ELDHER, M108-Oxidation, M111-Oxidation , C116-Dioxidation, M121-Oxidation
Precursor ion: +4
Xcorr: 1.76

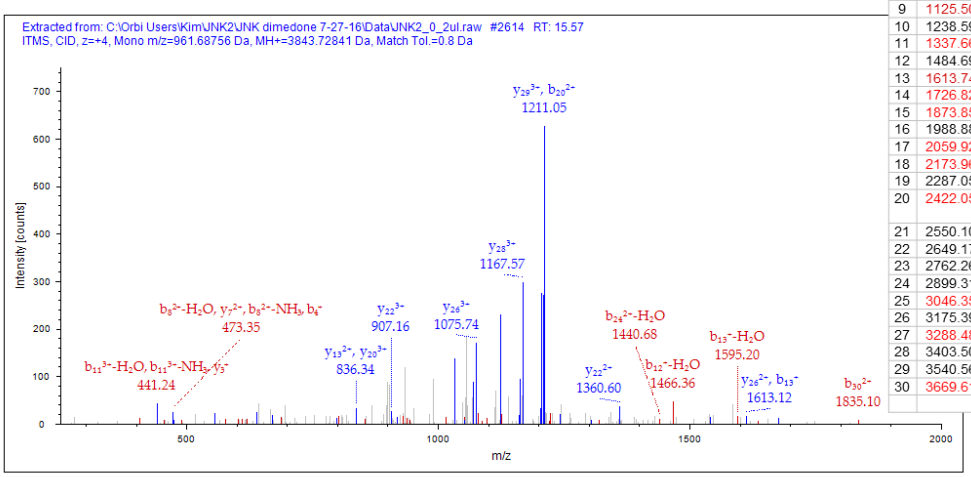

	b+	Seq.	y+	
1	102.05496	T		
2	215.13903	L	3742.67453	30
3	344.18163	E	3629.59046	29
4	473.22423	E	3500.54786	28
5	620.29265	F	3371.50526	27
6	748.35123	Q	3224.43684	26
7	863.37818	D	3096.37826	25
8	962.44660	V	2981.35131	24
9	1125.50992	Y	2882.28289	23
10	1238.59399	L	2719.21957	22
11	1337.66241	V	2606.13550	21
12	1484.69782	M-Oxidation	2507.06708	20
13	1613.74042	E	2360.03166	19
14	1726.82449	L	2230.98906	18
15	1873.85991	M-Oxidation	2117.90499	17
16	1988.88686	D	1970.86958	16
17	2059.92398	A	1855.84263	15
18	2173.96691	N	1784.80551	14
19	2287.05098	L	1670.76258	13
20	2422.05000	C-Dioxidation	1557.67851	12
21	2550.10858	Q	1422.67949	11
22	2649.17700	V	1294.62091	10
23	2762.26107	I	1195.55249	9
24	2899.31998	H	1082.46842	8
25	3046.35539	M-Oxidation	945.40951	7
26	3175.39799	E	798.37409	6
27	3288.48206	L	669.33149	5
28	3403.50901	D	556.24742	4
29	3540.56792	H	441.22047	3
30	3669.61052	E	304.16156	2
		R	175.11896	1

C.

TLEEFQDVYLVMELM[111]DANLC[116]QVIHM[121]ELDHER, M111-Oxidation, C116-Trioxidation, M121-Oxidation
Precursor ion: +4
Xcorr: 1.67

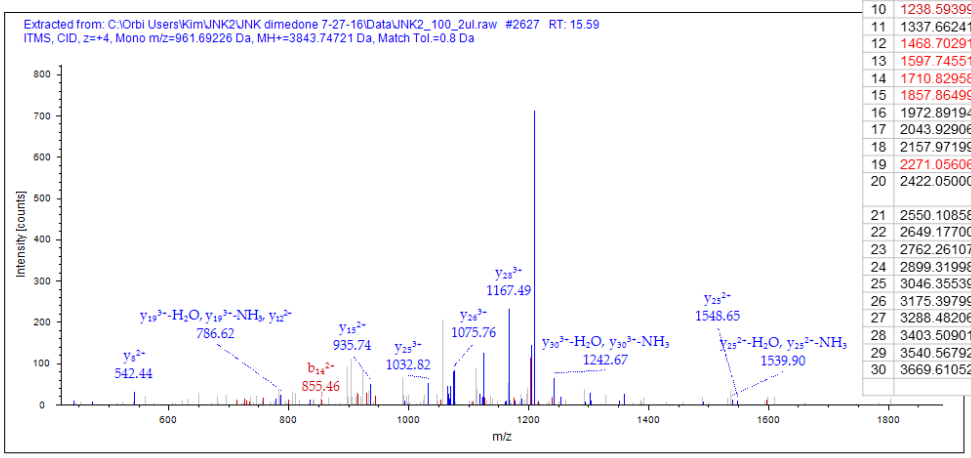

	b+	Seq.	y+	
1	102.05496	T		
2	215.13903	L	3742.67453	30
3	344.18163	E	3629.59046	29
4	473.22423	E	3500.54786	28
5	620.29265	F	3371.50526	27
6	748.35123	Q	3224.43684	26
7	863.37818	D	3096.37826	25
8	962.44660	V	2981.35131	24
9	1125.50992	Y	2882.28289	23
10	1238.59399	L	2719.21957	22
11	1337.66241	V	2606.13550	21
12	1468.70291	M	2507.06708	20
13	1597.74551	E	2376.02658	19
14	1710.82958	L	2246.98398	18
15	1857.86499	M-Oxidation	2133.89991	17
16	1972.89194	D	1986.86449	16
17	2043.92906	A	1871.83754	15
18	2157.97199	N	1800.80042	14
19	2271.05606	L	1686.75749	13
20	2422.05000	C-Trioxidation	1573.67342	12
21	2550.10858	Q	1422.67949	11
22	2649.17700	V	1294.62091	10
23	2762.26107	I	1195.55249	9
24	2899.31998	H	1082.46842	8
25	3046.35539	M-Oxidation	945.40951	7
26	3175.39799	E	798.37409	6
27	3288.48206	L	669.33149	5
28	3403.50901	D	556.24742	4
29	3540.56792	H	441.22047	3
30	3669.61052	E	304.16156	2
		R	175.11896	1

D.

SDC[163]TLKILDFGLAR, C163-Dioxidation
Precursor Ion: +3
XCorr: 1.17

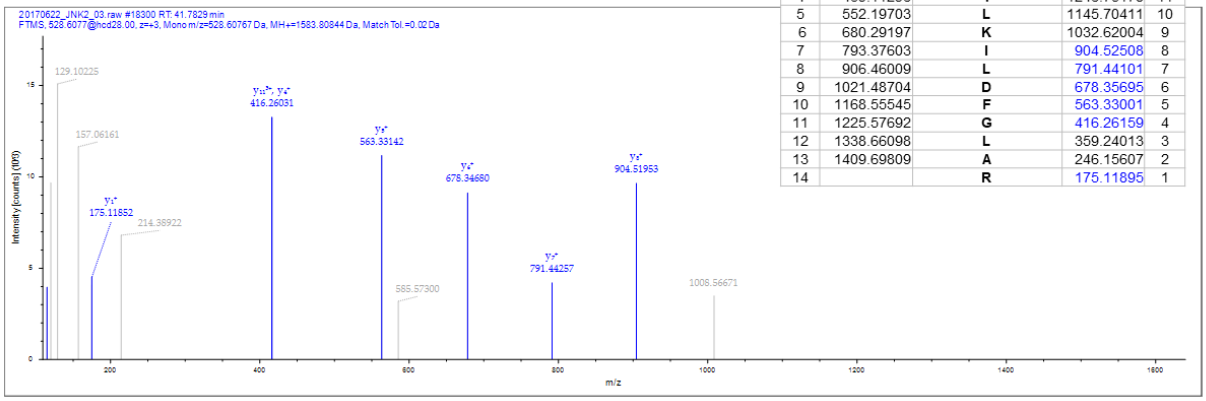

	b+	Seq.	y+	
1	88.03931	S		14
2	203.06626	D	1496.77774	13
3	338.06528	C-Dioxidation	1381.75080	12
4	439.11296	T	1246.75178	11
5	552.19703	L	1145.70411	10
6	680.29197	K	1032.62004	9
7	793.37603	I	904.52508	8
8	906.46009	L	791.44101	7
9	1021.48704	D	678.35695	6
10	1168.55545	F	563.33001	5
11	1225.57692	G	416.26159	4
12	1338.66098	L	359.24013	3
13	1409.69809	A	246.15607	2
14		R	175.11895	1

E.

TAC[177]TNFM[181]M[182]TPYVVTR, M181-Oxidation, M182-Oxidation, C177-Dioxidation
Precursor Ion: +2
XCorr:1.64

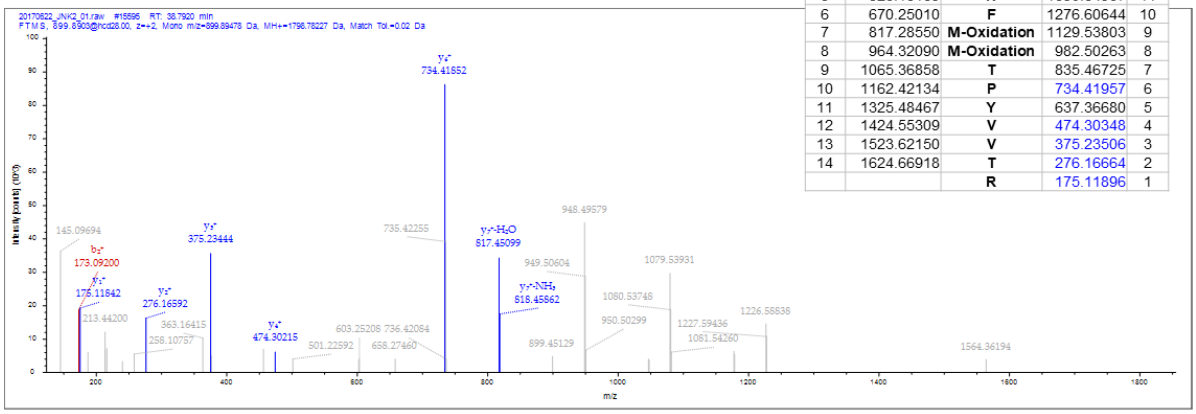

	b⁺	Seq.	y⁺	
1	102.05496	T		
2	173.09208	A	1697.73318	14
3	308.09108	C-Dioxidation	1626.69606	13
4	409.13876	T	1491.69705	12
5	523.18169	N	1390.64937	11
6	670.25010	F	1276.60644	10
7	817.28550	M-Oxidation	1129.53803	9
8	964.32090	M-Oxidation	982.50263	8
9	1065.36858	T	835.46725	7
10	1162.42134	P	734.41957	6
11	1325.48467	Y	637.36680	5
12	1424.55309	V	474.30348	4
13	1523.62150	V	375.23506	3
14	1624.66918	T	276.16664	2
		R	175.11896	1

F.

TAC[177]TNFM[181]M[182]TPYVVTR, M181-Oxidation, M182-Oxidation, C177-Trioxidation
Precursor Ion: +2
XCorr: 1.60

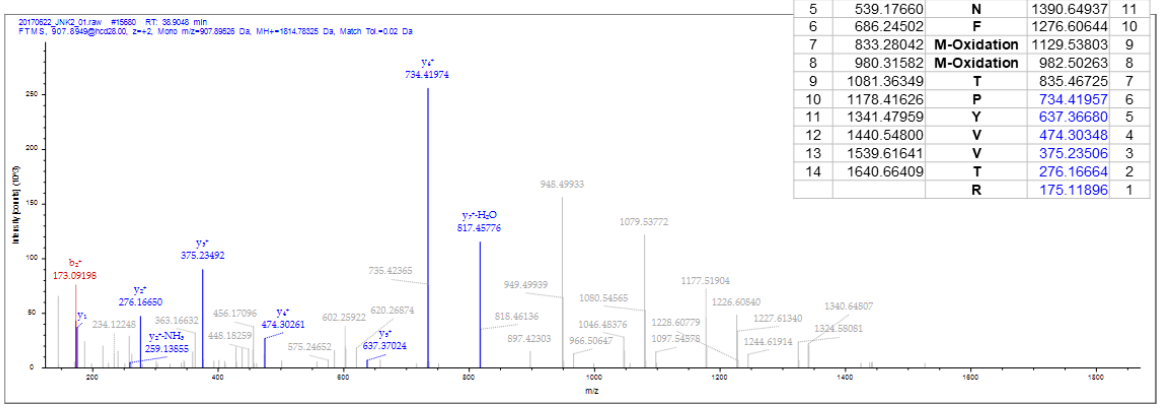

	b⁺	Seq.	y⁺	
1	102.05496	T		
2	173.09208	A	1713.72809	14
3	324.08600	C-Trioxidation	1642.69098	13
4	425.13368	T	1491.69705	12
5	539.17660	N	1390.64937	11
6	686.24502	F	1276.60644	10
7	833.28042	M-Oxidation	1129.53803	9
8	980.31582	M-Oxidation	982.50263	8
9	1081.36349	T	835.46725	7
10	1178.41626	P	734.41957	6
11	1341.47959	Y	637.36680	5
12	1440.54800	V	474.30348	4
13	1539.61641	V	375.23506	3
14	1640.66409	T	276.16664	2
		R	175.11896	1

G.

ENVDIWSVGC[213]IMGELVKGC[222]VIFQGTDHIDQWNK, C213-Trioxidation, M215-Oxidation, C222-Trioxidation
Precursor ion: +4
Xcorr: 0.54

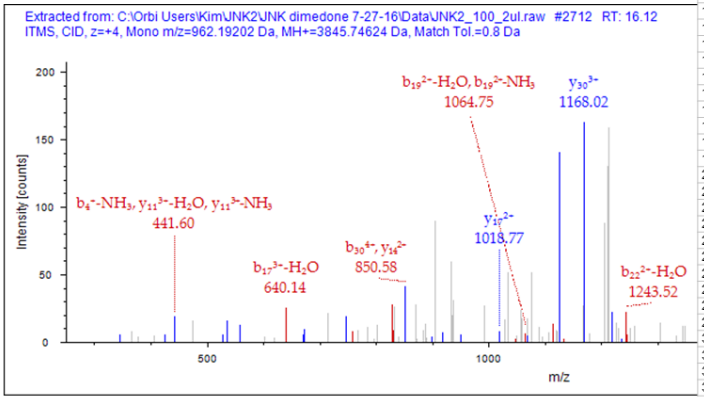

	b+	b2+	b4+	Seq.	y2+	y3+	
1	130.04988	44.02148	33.26793	E			33
2	244.09281	82.03579	61.77866	N	1858.85520	1239.57256	32
3	343.16123	115.05859	86.54576	V	1801.83374	1201.55825	31
4	458.18818	153.40091	115.30250	D	1752.29953	1168.53544	30
5	571.27225	191.09560	143.57352	I	1694.78605	1130.19313	29
6	757.35157	253.12204	190.09335	W	1638.24402	1092.49844	28
7	844.38360	282.13272	211.85136	S	1545.20436	1030.47200	27
8	943.45202	315.15552	236.61846	V	1501.68834	1001.46132	26
9	1000.47349	334.16268	250.87383	G	1452.15413	968.43851	25
10	1151.46742	384.49399	288.62231	C-Trioxidation	1423.64340	949.43136	24
11	1264.55149	422.18868	316.89333	I	1348.14643	899.10004	23
12	1411.58691	471.20049	353.65218	M-Oxidation	1291.60439	861.40535	22
13	1468.60838	490.20764	367.90755	G	1218.08669	812.39355	21
14	1597.65098	533.22184	400.16820	E	1189.57595	793.38639	20
15	1710.73505	570.91653	428.43922	L	1125.05465	750.37219	19
16	1809.80347	603.93934	453.20632	V	1068.51262	712.67750	18
17	1937.89844	646.63766	485.23007	K	1018.97841	679.65470	17
18	1994.91991	665.64482	499.48543	G	954.93092	636.95637	16
19	2145.91384	715.97613	537.23392	C-Trioxidation	926.42019	617.94922	15
20	2244.98226	748.99894	562.00102	V	850.92322	567.61790	14
21	2358.06633	786.69363	590.27204	I	801.38901	534.59510	13
22	2505.13475	835.71643	627.03914	F	744.84697	496.90041	12
23	2633.19333	878.40263	659.05379	Q	671.31276	447.87760	11
24	2690.21480	897.40978	673.30916	G	607.28347	405.19141	10
25	2791.26248	931.09234	698.57108	T	578.77274	386.18425	9
26	2906.28943	969.43466	727.32781	D	528.24890	352.50169	8
27	3043.34834	1015.12096	761.59254	H	470.73542	314.15937	7
28	3156.43241	1052.81565	789.86356	I	402.20597	268.47307	6
29	3271.45936	1091.15797	818.62030	D	345.66393	230.77838	5
30	3399.51794	1133.84416	850.63494	Q	288.15046	192.43606	4
31	3585.59726	1195.87060	897.15477	W	224.12117	149.74987	3
32	3699.64019	1233.88491	925.66550	N	131.08151	87.72343	2
33				K	74.06004	49.70912	1

H.

GC[222]VIFQGTDHIDQWNK, C222-Dioxidation
Precursor Ion: +3,
XCorr: 4.16

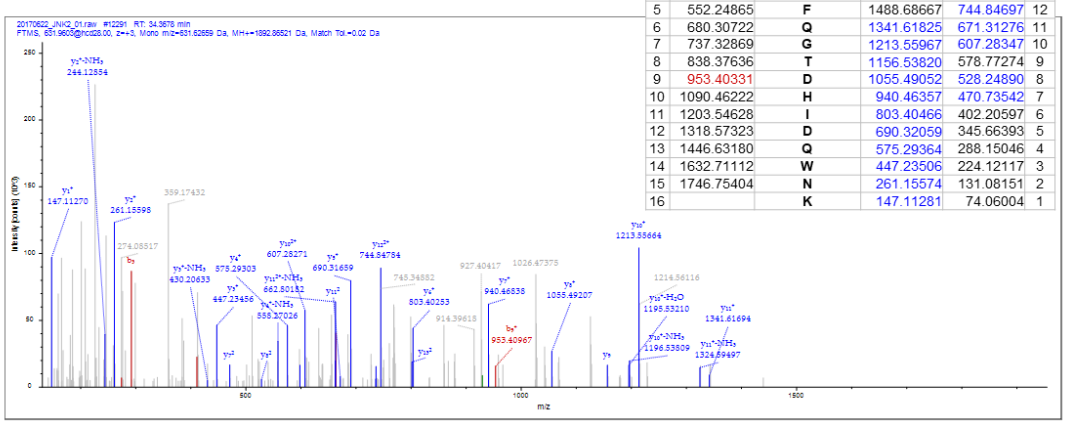

	b+	Seq.	y+	y2+	
1	58.02874	G		954.93092	16
2	193.02775	C-Dioxidation	1835.83811	926.42019	15
3	292.09617	V	1700.83909	850.92322	14
4	405.18023	I	1601.77074	801.38901	13
5	552.24865	F	1488.68667	744.84697	12
6	680.30722	Q	1341.61825	671.31276	11
7	737.32869	G	1213.55967	607.28347	10
8	838.37636	T	1156.53820	578.77274	9
9	953.40331	D	1055.49052	528.24890	8
10	1090.46222	H	940.46357	470.73542	7
11	1203.54628	I	803.40466	402.20597	6
12	1318.57323	D	690.32059	345.66393	5
13	1446.63180	Q	575.29364	288.15046	4
14	1632.71112	W	447.23506	224.12117	3
15	1746.75404	N	261.15574	131.08151	2
16		K	147.11281	74.06004	1

I.

GC_{222}VIFQGTDHIDQWNK, C222-Trioxidation
Precursor Ion: +2
XCorr: 2.42

	b+	Seq.	y+	y2+	
1	58.02874	G			16
2	209.02267	C-Trioxidation	1851.83302	926.42019	15
3	308.09108	V	1700.83909	850.92322	14
4	421.17515	I	1601.77074	801.38901	13
5	568.24356	F	1488.68667	744.84697	12
6	696.30214	Q	1341.61825	671.31276	11
7	753.32360	G	1213.55967	607.28347	10
8	854.37128	T	1156.53820	578.77274	9
9	969.39822	D	1055.49052	528.24890	8
10	1106.45713	H	940.46357	470.73542	7
11	1219.54120	I	803.40466	402.20597	6
12	1334.56814	D	690.32059	345.66393	5
13	1462.62672	Q	575.29364	288.15046	4
14	1648.70603	W	447.23506	224.12117	3
15	1762.74896	N	261.15574	131.08151	2
16		K	147.11281	74.06004	1

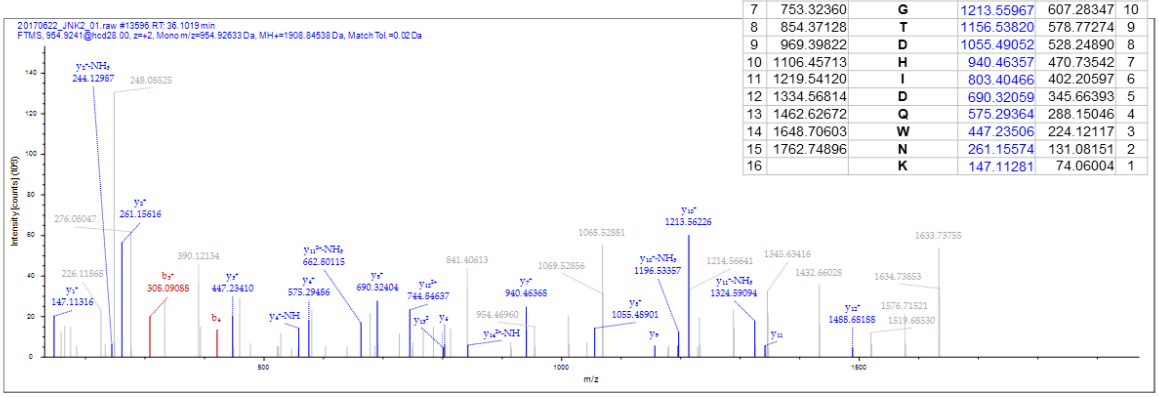

Fig. S6. Positive ion MS2 spectrum of the (A) C6-SO_2H, (B) C116-SO_2H, (C) C116-SO_3H, (D) C163-SO_2H (E) C177-SO_2H (F) C177-SO_3H (G) C213-SO_3H & C222-SO_3H (H) C222-SO_3H and (I) C222-SO_2H peptides. Spectra B, C, and G were obtained after treating recombinant His-tagged JNK2α2 with or without 5 additions of 100 µM H_2O_2 in the presence of 5 mM DTT and 5 mM dimedone (Table SI, Experiment 1). Free thiols were blocked with IAM prior to digestion with trypsin. The resulting peptides were analyzed by LC-MS/MS using an Accela Open UPLC coupled to a Thermo Scientific Orbi-trap LTQ XL mass spectrometer. Spectra A, D, E, F, H, and I were obtained after incubating pre-reduced His-tagged JNK2α2 with or without 100 µM H_2O_2 in the presence of 5 mM dimedone (Table SI, Experiment 2). Free thiols were blocked with MSBT prior to digestion with trypsin. The resulting peptides were analyzed by LC-MS/MS using Q Exactive HF hybrid quadrupole-Orbitrap mass spectrometer (Thermo Scientific) coupled to a Dionex Ultimate-3000 nano-UPLC system (Thermo Scientific) and a Nanospray Flex Ion Source (Thermo Scientific).

A.

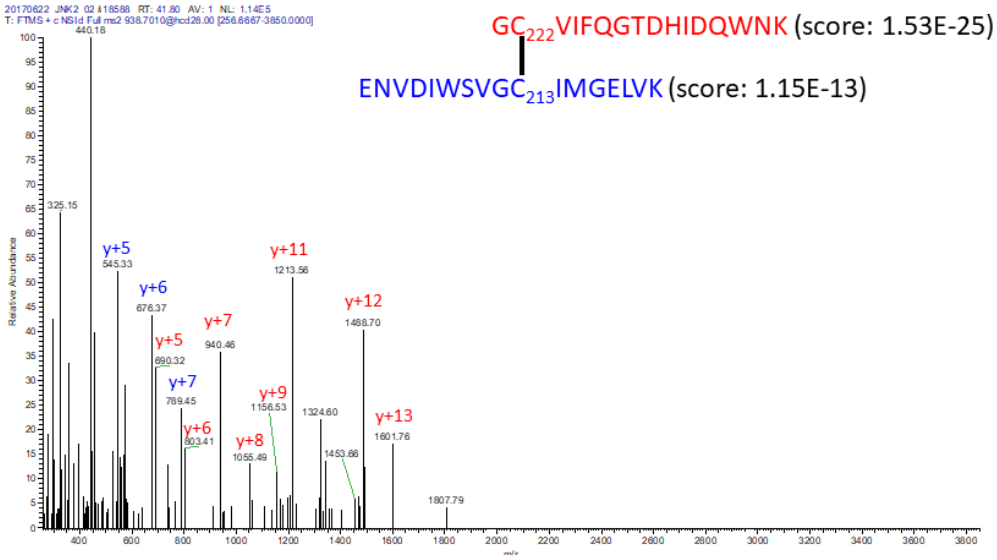

B.

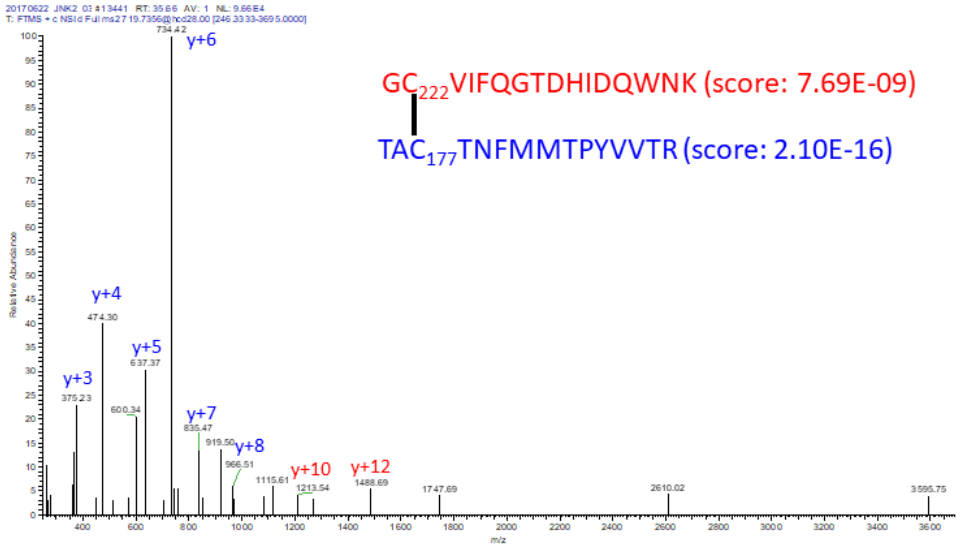

Fig. S7. Positive ion MS2 spectrum of the (A) C222-C213 and (B) C222-C177 disulfide bonded peptides in JNKα2. Spectra were obtained after incubating pre-reduced His-tagged JNK2α2 with 100 μM H_2O_2 in the presence of 5 mM dimedone. Free thiols were blocked with MSBT prior to digestion with trypsin. The resulting peptides were analyzed by LC-MS/MS using Q Exactive HF hybrid quadrupole-Orbitrap mass spectrometer (Thermo Scientific) coupled to a Dionex Ultimate-3000 nano-UPLC system (Thermo Scientific) and a Nanospray Flex Ion Source (Thermo Scientific).

References

1. Sievers, F., Wilm, A., Dineen, D., Gibson, T. J., Karplus, K., Li, W., Lopez, R., McWilliam, H., Remmert, M., Soding, J., Thompson, J. D., and Higgins, D. G. (2011)

Fast, scalable generation of high-quality protein multiple sequence alignments using Clustal Omega. *Mol Syst Biol* **7**, 539
2. Kallunki, T., Su, B., Tsigelny, I., Sluss, H. K., Derijard, B., Moore, G., Davis, R., and Karin, M. (1994) JNK2 contains a specificity-determining region responsible for efficient c-Jun binding and phosphorylation. *Genes Dev* **8**, 2996-3007
3. Nitta, R. T., Chu, A. H., and Wong, A. J. (2008) Constitutive activity of JNK2 alpha2 is dependent on a unique mechanism of MAPK activation. *J Biol Chem* **283**, 34935-34945